A 28 GHz Band Compact LTCC Filtering Antenna with Extracted-Pole Unit for Dual Polarization

Kaoru SUDO[†a], *Member*, **Ryo MIKASE**[†], **Yoshinori TAGUCHI**[†], *Nonmembers*, **Koichi TAKIZAWA**[†], **Yosuke SATO**[†], *Members*, **Kazushige SATO**[†], **Hisao HAYAFUJI**[†], *Nonmembers*, *and* **Masataka OHIRA**[††], *Senior Member*

SUMMARY   This paper proposes a dual-polarized filtering antenna with extracted-pole unit (EPU) using LTCC substrate. The EPU realizes the high skirt characteristic of the bandpass filter with transmission zeros (TZs) located near the passband without cross coupling. The filtering antenna with EPU is designed and fabricated in 28 GHz band for 5G Band-n257 (26.5–29.5 GHz). The measured S_{11} is less than -10.6 dB in Band-n257, and the isolation between two ports for dual polarization is greater than 20.0 dB. The measured peak antenna gain is 4.0 dBi at 28.8 GHz and the gain is larger than 2.5 dBi in Band-n257. The frequency characteristics of the measured antenna gain shows the high skirt characteristic out of band, which are in good agreement with electromagnetic (EM)-simulated results.
key words: mobile communication, millimeter wave antennas, bandpass filters (BPFs), transmission zeros (TZs)

1.   Introduction

Millimeter waves communication is one of the key technologies for the 5th generation communications system (5G). The specifications of 5G have been discussed in 3GPP and the requirements on equivalent isotropic radiated power (EIRP), sensitivities, and spurious emission have been determined in both 28 GHz and 39 GHz bands for user equipment (UE) and base station [1]. To address a rapid growing data traffic, massive MIMO and beam forming are important technologies. Antenna-Array-Integrated Modules (AiMs) have been employed in the MIMO antenna units with a tiled configuration for base station application.

The AiMs of millimeter wave bands are actively developed for 5G base station [2]–[6]. Figure 1 shows the structure of the AiM for 5G base station. The array antenna is integrated in LTCC substrate, and RFIC and other components are mounted on the opposite side of antennas. The photographs of the AiM examples are shown in Fig. 2. The dual-polarization antenna is used for the AiM of 5G millimeter waves to realize the polarization MIMO communication [7]–[10].

The spurious emissions from the antenna units, such as leaks from local oscillators and harmonics from power amplifier (PA) outputs should be suppressed not to interfere
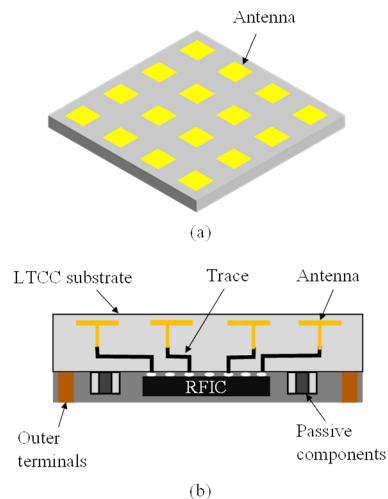
Fig. 1   Basic configuration of AiM: (a) structure, (b) cross section.
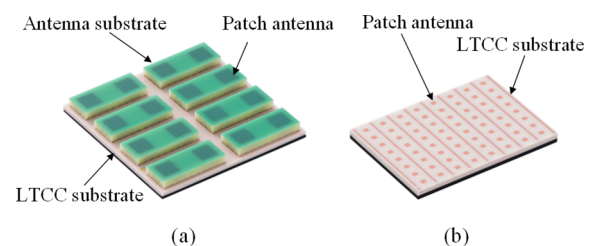
Fig. 2   Examples of AiM: (a) AiM for 5G base station, (b) AiM for 60 GHz backhaul.
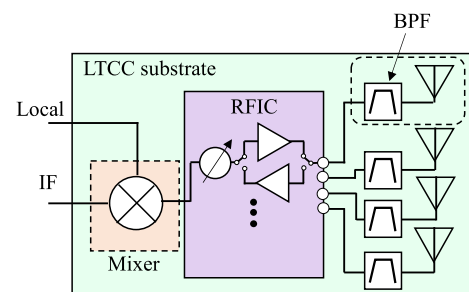
Fig. 3   Block diagram of AiM.

with signals at other bands [11]. The 28 GHz array antenna with a bandpass filter (BPF) in front of the power divider has been proposed [12]. To realize beam forming in the array antenna, a BPF should be added to each antenna element. Figure 3 shows the block diagram of the AiM. IF signals

are input to the mixer in RFIC and the BPFs are integrated in the LTCC substrate between the RFIC and antennas. A compact BPF with the antenna is necessary for realizing this structure.

It is a conventional design method that the filter and the antenna are designed separately, and they are connected by $50\,\Omega$ line [13], [14]. In a recent co-design approach of the antenna and the BPF, the filtering antenna is constructed by replacing the Nth resonator of an Nth-order BPF with a radiation element [15]–[22].

In this paper, a new 28 GHz band dual-polarized LTCC filtering antenna with extracted-pole unit (EPU) [23], which realizes transmission zeros (TZs) without cross coupling, is proposed. The EPU for the filtering antenna makes it possible to remove the intersection between two feeding lines and two cross-coupling lines, which leads to a simple structure. The effectiveness of the proposed filtering antenna with the EPU is verified through design, fabrication, and measurements.
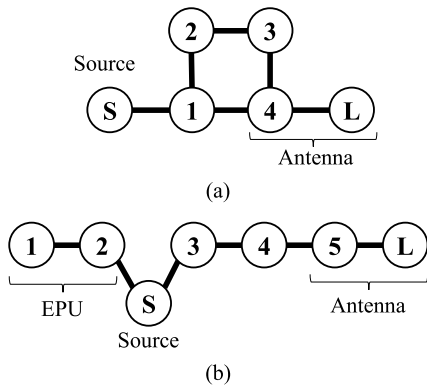
Fig. 4 Schematic topology of filtering antenna: (a) with cross coupling, (b) with EPU.
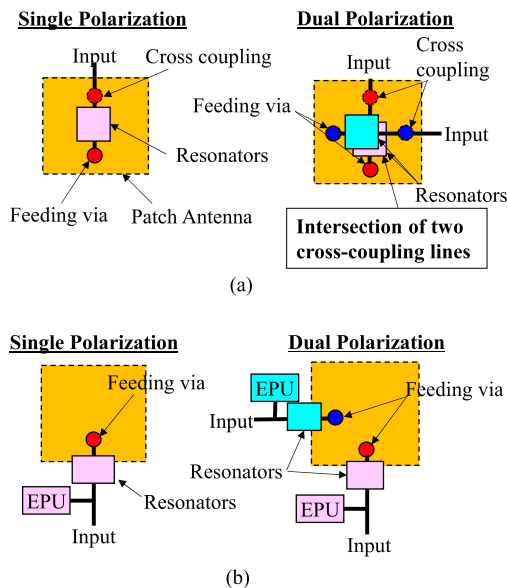
Fig. 5 Basic structure of filtering antenna: (a) with cross coupling, (b) with EPU.

2. Proposed Filtering Antenna

Figure 4 shows the schematic topology of two types of the single-feed compact filtering antenna. One is the filtering antenna with cross coupling, and another is the filtering antenna with EPU. To provide the high skirt characteristic, a filter with cross coupling between non-adjacent resonators is used [24]–[26]. The cross coupling between the resonator and the radiation element realizes TZs located near the passband, providing the high skirt characteristic as the BPF. Figure 4 (a) shows the topology of the filtering antenna with cross coupling. The 4th resonator is the radiation element, and the radiation element and the 1st resonator are coupled as cross coupling, so that there are the two-point feeds to the radiation element. Figure 5 (a) shows the basic structures of the single polarization and the dual polarization filtering antennas with cross coupling. The structure of the dual-polarized filtering antenna with cross coupling is difficult to realize because of a complicated intersection of two cross-coupling lines and two feeding lines coupled to a single radiation element.

Figure 4 (b) shows the topology of the filtering antenna with EPU. The EPU is composed of the 1st and the 2nd resonators, while the 5th resonator is the radiation element. The EPU can improve the skirt characteristic of the BPF with TZs without cross coupling [27], [28]. Figure 5 (b) shows the structures of the single polarization and the dual polarization filtering antennas with EPU. No cross couplings enable us to easily realize a dual-feeding structure.

3. Design of Filtering Antenna with EPU

The filtering antenna with EPU is designed in 28 GHz band
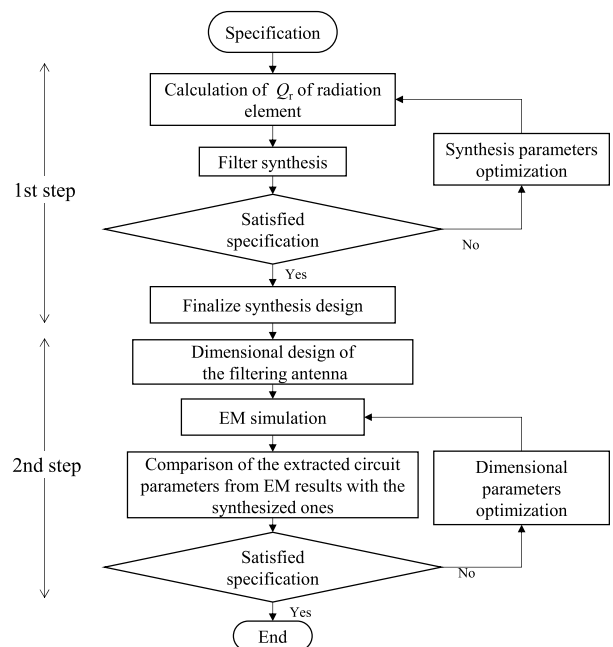
Fig. 6 Design flowchart of the filtering antenna.
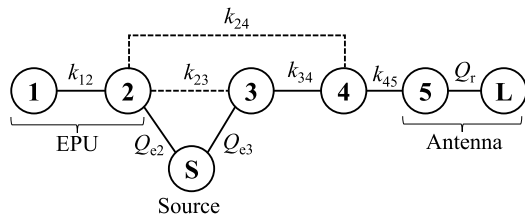
Fig. 7 Schematic topology of filtering antenna with EPU.

Table 1 Synthesized circuit parameters of single-feed filtering antenna with EPU. (Diagonal elements are resonant frequencies in GHz. Couplings with source are external Q factor, while coupling with load is radiation Q factor of radiation element. Other non-diagonal elements are coupling coefficients.).

	Source	R1	R2	R3	R4	R5	Load
S	0	0	1.36	8.66	0	0	0
R1	0	26.92	0.41	0	0	0	0
R2	1.36	0.41	26.76	0.08	0.06	0	0
R3	8.66	0	0.08	27.57	0.10	0	0
R4	0	0	0.06	0.10	27.91	0.10	0
R5	0	0	0	0	0.10	28.01	13.49
L	0	0	0	0	0	13.49	0
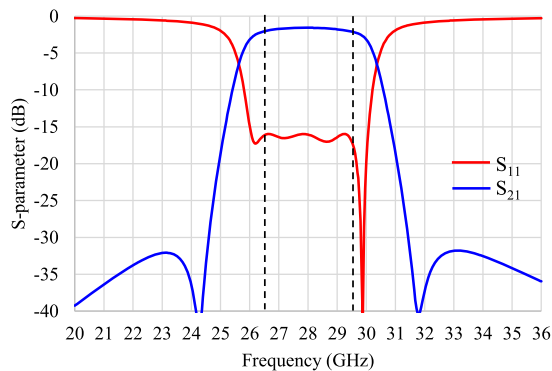
Fig. 8 Synthesized ideal S-parameter of filtering antenna with EPU.

for 5G Band-n257 (26.5–29.5 GHz). Figure 6 shows the design flowchart of the filtering antenna. As the 1st design step, the single-feed filtering antenna with EPU is synthesized by using the circuit topology shown in Fig. 7. The coupling coefficients k_{23} and k_{24} are added in this topology due to unexpected small couplings. The radiation Q factor (Q_r) of the radiation element is calculated from the S_{11} characteristic of the patch antenna model by using an electromagnetic (EM) simulator ANSYS® HFSS™ [21]. The value of the Q_r calculated by the EM-simulator is 13.49.

Table 1 shows the synthesized circuit parameters as the result of the synthesis parameter optimization. The synthesized circuit parameters are optimized to be realized S_{11} below −10 dB in the designed frequency band, except for Q_r that is determined by the structure of the radiation element. It is found from Table 1 that a strong coupling between source and 2nd resonator (external Q factor Q_{S2} = 1.36) as well as a strong one between 1st resonator and 2nd resonator

(coupling coefficient k_{12} = 0.41 for EPU) are necessary.

Figure 8 shows the synthesized ideal S-parameter of filtering antenna with EPU by using the circuit parameters of Table 1. Since the schematic topology is two port circuit, the synthesized ideal S-parameter is two port result. The port 1 is the source and the port 2 is the load. The S_{11} of the synthesized ideal S-parameter is below −15 dB in the designed frequency band.

4. Dimensional Design of Filtering Antenna with EPU

The dimensional parameters are designed by using an ANSYS® HFSS™, as the 2nd design step shown in Fig. 6. In the dimensional design, the single polarization filtering antenna is one port structure instead of two port circuit, because of the radiation element of the filtering antenna. We selected a LTCC material with relative permittivity ε_r = 6.6 and dielectric loss of tanδ = 0.005. The vector fitting method [29], [30] is used to extract the circuit parameters from the EM-simulated results. The dimensional parameters are optimized with comparing the extracted circuit parameters with the synthesized ones as shown in the 2nd step of Fig. 6 [9].

Two types of the filtering antenna are designed. The feeding structure of the radiation element is different between design A and B.

4.1 Design A

Figures 9 and 10 show the structure (design A) of filtering antenna with EPU. This filtering antenna is constructed in a LTCC substrate. The four resonators are $\lambda_g/4$ resonators with a shorted end to GND, where λ_g is the guided wavelength. The 1st, the 2nd, the 3rd and the 4th resonator are placed under the GND plane and the 5th resonator is over the GND plane. The 4th resonator and the 5th resonator are connected through the feeding via. The position of the feeding via is shifted in layer 7 because of the LTCC process. The total size of the four resonators (resonator unit) is 1.05 × 1.05 mm², which is smaller than the size of the radiation element of 1.81 × 1.81 mm².

Table 2 shows the dimensional parameters of the designed filtering antenna with EPU. To realize the abovementioned strong couplings, the 2nd resonator and the input line are overlapped. A coupling pad between the 1st resonator and the 2nd resonator is inserted to adjust the coupling coefficient k_{12}.

Figure 11 shows the EM-simulated S-parameter and antenna gain of filtering antenna with EPU. The antenna gain in boresight is simulated in the dimensional design, instead of S_{21} in the synthesized ideal S-parameter of filtering antenna. The EM-simulated S_{11} is less than −10.8 dB in Band-n257. The EM-simulated peak antenna gain is 4.1 dBi at 27.5 GHz and the gain is larger than 3.4 dBi in Band-n257. The EM-simulated antenna gain of the filtering antenna with EPU achieves the high skirt characteristics out of band with two TZs.
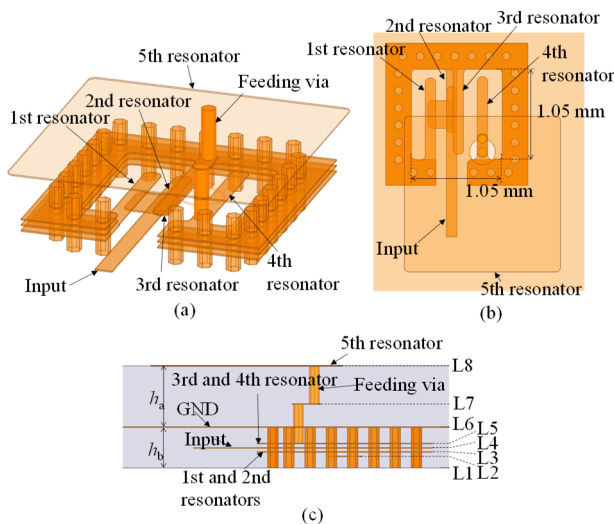
Fig. 9 Structure of single-feed filtering antenna with EPU (design A): (a) three-dimensional view, (b) top view, and (c) cross section.
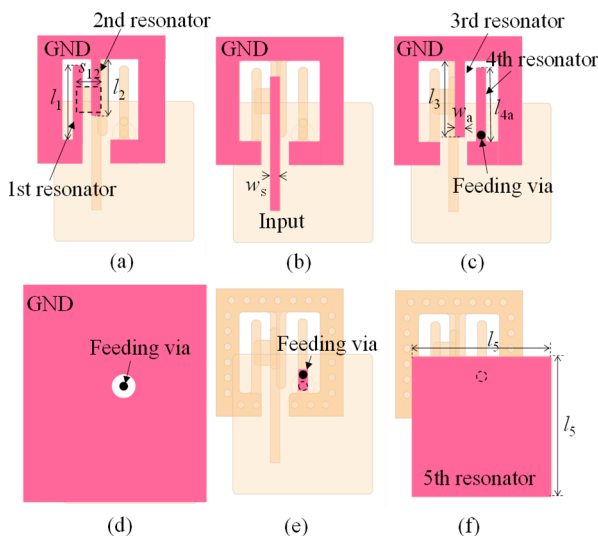
Fig. 10 Layout of single-feed filtering antenna with EPU (design A): (a) Layer 3, (b) Layer 4, (c) Layer 5, (d) Layer 6, (e) Layer 7, and (f) Layer 8.

Table 2 Dimensional parameters of filtering antenna with EPU (design A).

l_1	0.95	l_{4b}	-	s_{12}	0.31	
l_2	0.74	l_5	1.81	v_g	-	
l_3	0.99	w_a	0.12	h_a	0.57	
l_{4a}	0.96	w_s	0.12	h_b	0.38	Unit: mm

4.2 Design B

Figures 12 and 13 show the structure (design B) of the filtering antenna with EPU. The feeding structure to the radiation element of the design B is different from that of the design A. The 1st, the 2nd and the 3rd resonator are placed under the GND plane and same structure with these of the
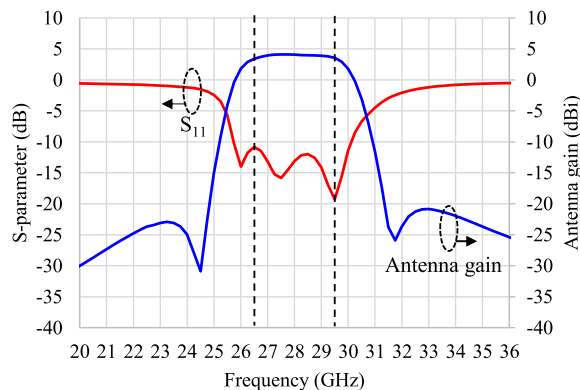
Fig. 11 EM-simulated S-parameter and antenna gain of filtering antenna with EPU (design A).

Table 3 Dimensional parameters of filtering antenna with EPU (design B).

l_1	0.97	l_{4b}	0.25	s_{12}	0.31	
l_2	0.79	l_5	1.68	v_g	0.36	
l_3	0.96	w_a	0.12	h_a	0.57	
l_{4a}	0.41	w_s	0.12	h_b	0.38	Unit: mm

design A. The structure of the 4th resonator is different from that of the design A. The 4th resonator consists of the vertical via hole and the planar patterns in layer 5 and layer 7, and it is folded from layer 5 to 7 across the GND plane for coupling to the radiation element, instead of feeding via of the design A. The reason of changing the feeding structure is the unexpected radiation from the feeding via of the design A in out of frequency band. Table 3 shows the dimensional parameters of the design B. These parameters of the design B are slightly different from the design A due to the difference of the 4th resonator.

Figure 14 shows the EM-simulated S-parameter and antenna gain of the design B. The EM-simulated S_{11} is less than −13.4 dB in Band-n257. The EM-simulated peak antenna gain is 4.1 dBi at 28.0 GHz and the gain is larger than 3.5 dBi in Band-n257. Figure 15 shows the EM-simulated antenna gains of the design A and B including out of frequency band. The unexpected radiation of design B in lower and higher frequency bands is suppressed as compared with that of the design A. Because the suppression of unexpected radiation in out of band of the design B is better than that of the design A, we use the structure of the design B as the dual polarization filtering antenna.

4.3 Dual-Polarized Filtering Antenna

As the final design step, the two resonator units are orthogonally located with each other so that they are coupled to a single radiation element for dual polarization, as shown in Fig. 16. The port 1 is connected to vertical polarization (V-pol.) antenna and the port 2 is connected to the horizontal polarization (H-pol.) antenna.

Figure 17 shows the EM-simulated S-parameter and
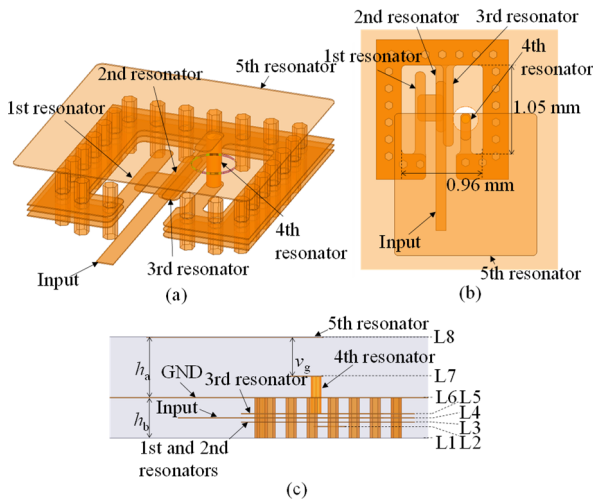
Fig. 12 Structure of single-feed filtering antenna with EPU (design B): (a) three-dimensional view, (b) top view, and (c) cross section.
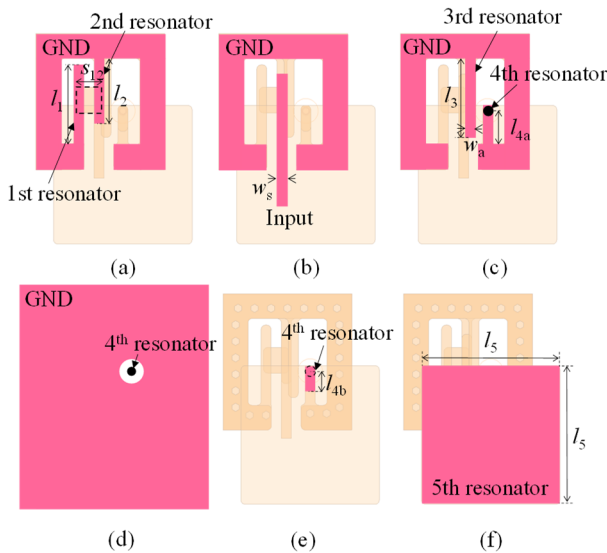
Fig. 13 Layout of single-feed filtering antenna with EPU (design B): (a) Layer 3, (b) Layer 4, (c) Layer 5, (d) Layer 6, (e) Layer 7, and (f) Layer 8.
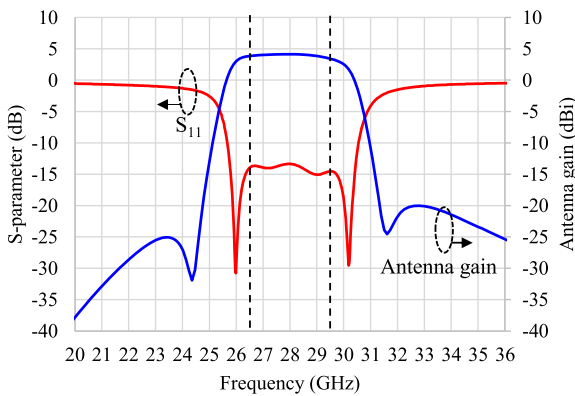
Fig. 14 EM-simulated S-parameter and antenna gain of filtering antenna with EPU (design B).
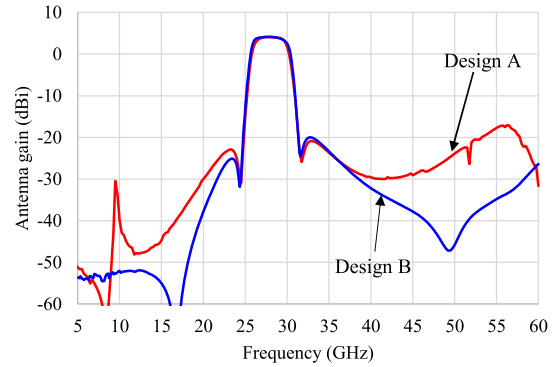
Fig. 15 EM-simulated antenna gain of filtering antenna with EPU (design A and B).
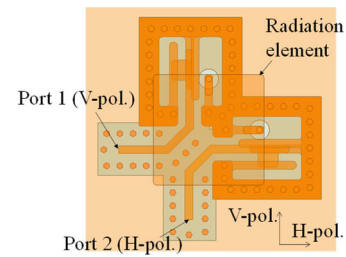
Fig. 16 Structure of dual-polarized filtering antenna with EPU.
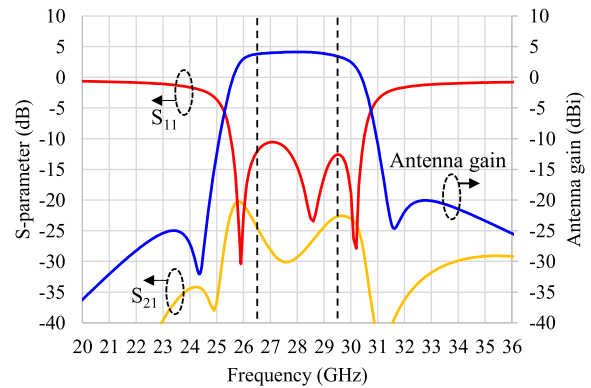
Fig. 17 EM-simulated S-parameter and antenna gain of filtering antenna with EPU (dual polarization).

antenna gain of the dual-polarized filtering antenna. The EM-simulated S_{11} is less than -10.6 dB in Band-n257. The EM-simulated maximum S_{21} is -22.7 dB at 29.5 GHz and the S_{21} is less than -20.0 dB in the designed bandwidth. The EM-simulated peak antenna gain is 4.1 dBi at 28.1 GHz and the gain is larger than 3.4 dBi in Band-n257.

5. Measurement Results

The designed dual-polarized filtering antenna is fabricated to verify experimentally the characteristics of the antenna. The fabricated antenna has two ports for dual polarization. Figure 18 shows the photograph of the fabricated dual-polarized filtering antenna with EPU. We fabricated two types of antennas; one has the probe pads to measure the
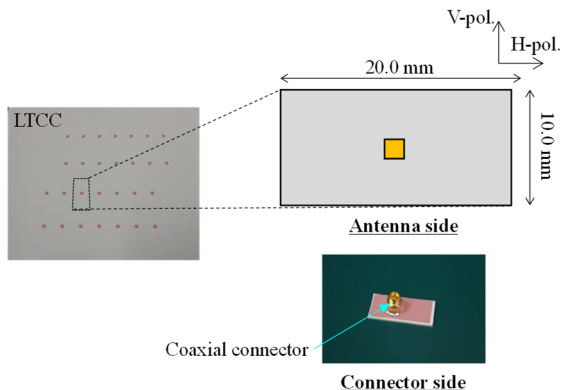
Fig. 18 Photograph of fabricated dual-polarized filtering antenna with EPU.
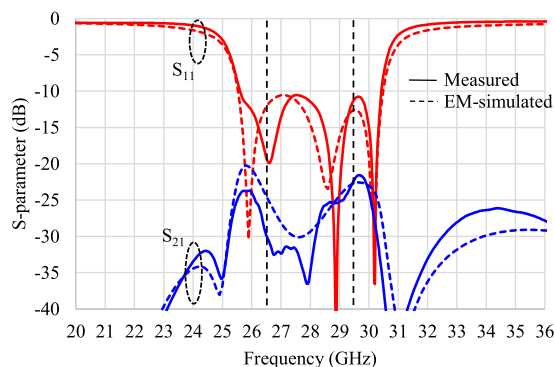
Fig. 19 EM-simulated and measured frequency responses of fabricated dual-polarized filtering antenna.

Fig. 20 Frequency characteristics of EM-simulated and measured antenna gain (horizontal polarization) of fabricated dual-polarized filtering antenna.
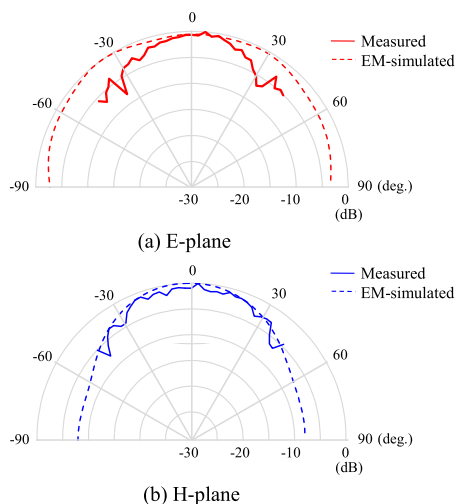
Fig. 21 EM-simulated and measured radiation patterns (horizontal polarization, at 28.0 GHz) of fabricated dual-polarized filtering antenna.

S-parameters, and another has a coaxial connector to measure the antenna gain in over the air. One port of the fabricated antenna for the measurement of the antenna gain is connected to the coaxial connector and another port is open, as shown in Fig. 18.

Figure 19 shows the comparison of frequency responses between the measured results and the EM-simulated results. The EM-simulated results are in good agreement with the measured results. The measured S_{11} is less than -10.6 dB in Band-n257. S_{21} is measured for verifying the isolation characteristic between two ports for dual polarizations. The measured maximum S_{21} is -21.6 dB at 29.7 GHz and the S_{21} is less than -20.0 dB in the designed bandwidth.

The frequency characteristic of antenna gain was evaluated with an over-the-air measurement in an anechoic chamber. Figure 20 shows the simulated and the measured antenna gain characteristics of the fabricated filtering antenna in boresight. The measured peak antenna gain is 4.0 dBi at 28.8 GHz and the gain is larger than 2.5 dBi in Band-n257. The measured antenna gain achieves the high skirt characteristics out of band, thanks to two TZs of the EPU. Figure 21 shows the EM-simulated and measured radiation patterns of the fabricated dual-polarized filtering antenna at 28.0 GHz. These results are normalized by the peak antenna gains, individually. The measured pattern of the E-plane is

different from the EM-simulated one, because of the effect of the fixture in radiation pattern measurement system.

6. Conclusion

In this paper, a 28 GHz band dual-polarized LTCC filtering antenna with EPU has been proposed. The EPU has realized the high skirt characteristic with TZs generated near the passband without cross coupling. We designed two types (design A and design B) of the filtering antenna with EPU in 28 GHz band. Because the suppression of unexpected radiation in out of band of design B is better than that of design A, we designed and fabricated the structure of design B as the dual polarization filtering antenna. As the results of S-parameter measurement, the S_{11} has been less than -10.6 dB in Band-n257, and the isolation between two ports for dual polarization has been greater than 20.0 dB. The measured peak antenna gain in boresight has been larger than 2.5 dBi in Band-n257, and the peak gain has been 4.0 dBi at 28.8 GHz. The measured antenna gain has achieved the skirt characteristics out of band. The new

filtering antenna is expected to be used for the AiM of 5G base station.

References

[1] 3GPP standardization, http://www.3gpp.org/

[2] J. Dunworth, B.-H. Ku, Y.-C. Ou, D. Lu, P. Mouat, A. Homayoun, K. Chakraborty, A. Arnett, G. Liu, T. Segoria, J. Lerdworatawee, J.W. Park, H.-C. Park, H. Hedayati, A. Tassoudji, K. Douglas, and V. Aparin, "28 GHz phased array transceiver in 28 nm bulk CMOS for 5G prototype user equipment and base stations," Proc. IEEE MTT-S Int. Microw. Symp., pp.1330–1333, June 2018.

[3] R. Valkonen, "Compact 28-GHz phased array antenna for 5G access," Proc. IEEE MTT-S Int. Microw. Symp., pp.1334–1337, June 2018.

[4] S. Yamaguchi, H. Watanabe, H. Yoshioka, Y. Morimoto, H. Nakamizo, K. Tsutsumi, S. Shinjo, S. Uchida, A. Okazaki, T. Fukasawa, and N. Yoneda, "Development of 28GHz band massive MIMO antenna RF frontend module for 5G," Proc. IEEE Trans. Antennas Propag.-S Int. Symp., pp.629–630, July 2018.

[5] X. Gu, D. Liu, C. Baks, O. Tageman, B. Sadhu, J. Hallin, L. Rexberg, P. Parida, Y. Kwark, and A. Valdes-Garcia, "Development, implementation, and characterization of a 64-element dual-polarized phased-array antenna module for 28-GHz high-speed data communications," IEEE Trans. Microw. Theory Tech., vol.67, no.7, pp.2975–2984, July 2019.

[6] X. Gu, D. Liu, Y. Suto, Y. Tojo, Y. Hasegawa, C. Baks, N. Guan, A. Paidimarri, B. Sadhu, and A. Valdes-Garcia, "Novel phased array antenna-in-package development and active module demonstration for 5G millimeter-wave wireless communication," Proc. 2021 IEEE 71st Electronic Components and Technology Conference (ECTC), pp.1144–1149, June 2021.

[7] Y. Wang and D. Piao, "A compact size dual-polarized high-gain resonant cavity antenna at 28 GHz," Proc. International Applied Computational Electromagnetics Society Symposium (ACES), pp.1–2, March 2017.

[8] H. Xia, T. Zhang, L. Li, and F.-C. Zheng, "A low-cost dual-polarized 28 GHz phased array antenna for 5G communications," Proc. International Workshop on Antenna Technology (iWAT), pp.1–4, March 2018.

[9] J. Guo, F. Liu, L. Zhao, and Y. Yin, "A dual-polarized patch antenna with high isolation," Proc. 2019 International Symposium on Antennas and Propagation (ISAP), pp.1–3, Oct. 2019.

[10] A. Dadgarpour, N. Bayat-Makou, M.A. Antoniades, A.A. Kishk, and A. Sebak, "A dual-polarized magnetoelectric dipole array based on printed ridge gap waveguide with dual-polarized split-ring resonator Lens," IEEE Trans. Antennas Propag., vol.68, no.5, pp.3578–3585, May 2020.

[11] K. Andersson, "mm-Wave front-end challenges for 5G base stations," IEEE MTT-S Int. Microwave Symp., Workshop WFB-2, June 2018.

[12] Y. Feng, B. Yang, Y. Ji, and J. Zhou, "A 28 GHz millimeter-wave antenna array with SIW feeding network," Proc. International Conference on Microwave and Millimeter Wave Technology (ICMMT), pp.1–3, May 2019.

[13] K. Sudo, K. Onaka, K. Hirose, Y. Hasegawa, R. Komura, Y. Yamada, T. Hiratsuka, M. Koshino, and H. Hayafuji, "28 GHz antenna-array-integrated module with built-in filters in LTCC substrate," Proc. 2019 Asia-Pacific Microwave Conf. (APMC), pp.1041–1043, Dec. 2019.

[14] K. Sudo, K. Onaka, K. Hirose, Y. Hasegawa, R. Komura, Y. Yamada, and H. Hayafuji, "28 GHz array antenna with built-In filters in multilayered LTCC substrate," Proc. 2019 International Symposium on Antennas and Propagation (ISAP), pp.1–4, Oct. 2019.

[15] F. Queudet, I. Pele, B. Froppier, Y. Mahe, and S. Toutain, "Integration of pass-band filters in patch antennas," Proc. 32nd European Microwave Conf. (EuMC), pp.685–688, Sept. 2002.

[16] H. Cheng, Y. Yusuf, and X. Gong, "Vertically integrated three-pole filter/antennas for array applications," IEEE Antennas and Wireless Propagat. Lett., vol.10, pp.278–281, Jan. 2011.

[17] Y. Yusuf and X. Gong, "Compact low-loss integration of high-Q 3-D filters wih highly efficient antennas," IEEE Trans. Microw. Theory Tech., vol.59, no.4, pp.857–865, April 2011.

[18] W.-J. Wu, Y.-Z. Yin, S.-L. Zuo, Z.-Y. Zhang, and J.-J. Xie, "A new compact filter-antenna for modern wireless communication systems," IEEE Antennas and Wireless Propagat. Lett., vol.10, pp.1131–1134, Oct. 2011.

[19] Y. Yusuf, H. Cheng, and X. Gong, "A seamless integration of 3-D vertical filters with highly efficient slot antennas," IEEE Trans. Antennas and Propagat., vol.59, no.11, pp.4016–4022, Nov. 2011.

[20] C. Yu, W. Hong, Z. Kuai, and H. Wang, "Ku-band linearly polarized omnidirectional planar filtenna," IEEE Antennas and Wireless Propagat. Lett., vol.11, pp.310–313, Jan. 2012.

[21] M. Ohira and Z. Ma, "An efficient design method of microstrip filtering antenna suitable for circuit synthesis theory of microwave bandpass filters," Proc. 2015 International Symposium on Antennas and Propagation (ISAP), pp.846–849, Nov. 2015.

[22] Y. Li, Z. Zhao, Z. Tang, and Y. Yin, "Differentially fed, dual-band dual-polarized filtering antenna with high selectivity for 5G sub-6 GHz base station applications," IEEE Trans. Antennas Propag., vol.68, no.4, pp.3231–3236, April 2020.

[23] K. Sudo, R. Mikase, Y. Taguchi, K. Takizawa, Y. Sato, K. Sato, H. Hayafuji, and M. Ohira, "A 28 GHz band dual-polarized LTCC filtering antenna with extracted-pole unit," Proc. 2022 Asia-Pacific Microwave Conf. (APMC), pp.306–308, Dec. 2022.

[24] R.J. Cameron, "General coupling matrix synthesis methods for Chebyshev filtering functions," IEEE Trans. Microw. Theory Tech., vol.47, no.4, pp.433–442, April 1999.

[25] K.-S. Chin, C.-C. Chang, C.-H. Chen, Z. Guo, D. Wang, and W. Che, "LTCC Multilayered Substrate-Integrated Waveguide Filter with Enhanced Frequency Selectivity for System-in-Package Applications," IEEE Trans. Components, Packaging and Manufacturing Technology, vol.4, no.4, pp.664–672, April 2014.

[26] S. Amari and U. Rosenberg, "New building blocks for modular design of elliptic and self-equalized filters," IEEE Trans. Microw. Theory Tech., vol.52, no.2, pp.721–736, Feb. 2004.

[27] T. Zhang, Z. Long, L. Zhou, M. Qiao, F. Hou, and M. Tian, "Realization of even transmission zeros for filter without cross-couplings," IEEE Trans. Microw. Theory Tech., vol.66, no.12, pp.5248–5259, Dec. 2018.

[28] Y. Zeng, Y. Yang, Y. Wu, M. Yu, J. Peng, and D. Liang, "Exploiting redundancy in direct synthesis for inline filters," IEEE Trans. Microw. Theory Tech., vol.69, no.10, pp.4489–4498, Oct. 2021.

[29] C.-K. Liao, C.-Y. Chang, and J. Lin, "A vector-fitting formulation for parameter extraction of lossy microwave filters," IEEE Microwave and Wireless Components Lett., vol.17, no.4, pp.277–279, April 2007.

[30] H. Hu and K.-L. Wu, "A generalized coupling matrix extraction technique for bandpass filters with uneven-Qs," IEEE Trans. Microw. Theory Tech., vol.62, no.2, pp.244–251, Feb. 2014.

Kaoru Sudo   received the B.E., M.E., and D.E. degrees from Tokyo Institute of Technology, Tokyo, Japan, in 2000, 2002, and 2005, respectively. He was a Research Fellow of the Japan Society for the Promotion of Science (JSPS) from 2004 to 2005. He joined Murata Manufacturing Co., Ltd. in 2006. His research interests include millimeter-wave array antenna and packaging. He received the IEICE Young Engineer Award in 2006, and Asia-Pacific Microwave Conference (APMC) 2022 Prize in 2022. He is a member of the IEICE.

Ryo Mikase   received the B.E. and M.E. degrees in Saitama University, Saitama, Japan, in 2018 and 2020, respectively. He joined Murata Manufacturing Co., Ltd. in 2020, and is currently working on development of microwave and millimeter wave filter.

Yoshinori Taguchi   received the B.E. and M.E. degrees from Doshisha University, Kyoto, Japan, in 1993, 1995, respectively. He joined Murata Manufacturing Co., Ltd. in 1995, and is currently engaged in research on the analysis and design of microwave and millimeter-wave filters.

Koichi Takizawa   received the B.S. degree from Saitama University, Saitama, Japan, in 1996 and M.S. degree from the University of Tokyo, Tokyo, Japan, in 1998. He worked at Mitsubishi Electric Corporation from 1998 to 2001. He joined Murata Manufacturing Co., Ltd. in 2001, and is currently working on research of microwave and millimeter wave wireless communications.

Yosuke Sato   received the B.E., M.E., and D.E. degrees in Electrical and Communications Engineering from Tohoku University, Japan in 2010, 2011, and 2015 respectively. From 2015 to 2016, He was a researcher in Tohoku University, Japan. From 2017 to 2020, he worked at NIDEC ELESYS CORPORATION, specializing automotive millimeter wave radar R&D. He is currently antenna engineer in Murata Manufacturing Co., Ltd. His research interests include millimeter-wave antenna design and phased array systems. He is a member of the IEICE.

Kazushige Sato   received the B.E. and M.E. degree from Tokyo University of Agriculture and Technology, Tokyo, Japan, in 1999 and 2001, respectively. He joined Murata Manufacturing Co., Ltd in 2001, and is currently working on development of microwave and millimeter wave wireless modules.

Hisao Hayafuji   received the B.E. degree from Doshisha University, Kyoto, Japan, in 1993. He joined Murata Manufacturing Co., Ltd. in 1993, and is currently working on development of microwave and millimeter wave wireless modules.

Masataka Ohira   received the B.E., M.E., and D.E. degrees from Doshisha University, Kyoto, Japan, in 2001, 2003 and 2006, respectively. From 2006 to 2010, he was with ATR Wave Engineering Laboratories, Kyoto, Japan, where he was engaged in the research and development of millimeter-wave antennas and small smart microwave antennas. He was a Visiting Researcher in ATR Wave Engineering Laboratories for 2010–2011. In 2010, he joined Saitama University, Saitama, Japan, where he is currently an Associate Professor. His current research activities are concerned with the analysis and design of microwave/millimeter-wave filters and antennas. Dr. Ohira is a member of the Institute of Electrical Engineers (IEE) of Japan, European Microwave Association (EuMA), and IEEE. He received the IEICE Young Engineer Award in 2005, IEEE AP-S Japan Chapter Young Engineer Award in 2012, IEEE MTT-S Japan Young Engineer Award, Michiyuki Uenohara Memorial Award in 2014, and IEICE Best Paper Award in 2018.